

weak intermediate vector boson.

We thank Dr. B. W. Lee and Dr. A. I. Sanda for helpful discussions.

*Work supported by the U. S. Energy Research and Development Administration.

†Present address: Carnegie-Mellon University, Pittsburgh, Penn. 15213.

‡On leave of absence from Institute for Nuclear Research, Warsaw, Poland.

¹F. Reines, H. W. Sobel, and H. S. Gurr, *Phys. Rev. Lett.* **32**, 180 (1974); S. Pakvasa and K. Tennakone, *Phys. Rev. Lett.* **28**, 1415 (1972); M. Nakagawa *et al.*, *Progr. Theor. Phys.* **30**, 727 (1963).

²S. Eliezer and D. A. Ross, *Phys. Rev. D* **10**, 3088 (1974).

³V. E. Barnes, *Phys. Lett.* **65B**, 174 (1976).

⁴90%-confidence-level upper limits on m_{ν_e} : K. Bergkvist, *Nucl. Phys.* **B39**, 317 (1972); and on m_{ν_μ} : A. R. Clark *et al.*, *Phys. Rev. D* **9**, 533 (1974).

⁵S. Parker, H. L. Anderson, and C. Rey, *Phys. Rev.* **133**, B768 (1964).

⁶For example, W. J. Marciano and A. I. Sanda, Rockefeller University Report No. C00-2232B-116 (to be published), and Benjamin Lee, private communication; also T. P. Cheng and Ling-Fong Li, *Phys. Rev. Lett.* **38**, 381 (1977); F. Wilczek and A. Zee, *Phys. Rev. Lett.* **38**, 531 (1977); J. D. Bjorken and S. Weinberg, *Phys. Rev. Lett.* **38**, 622 (1977); B. W. Lee and R. E. Shrock, Fermilab Report No. FERMLAB-Pub-77/21-THY, 1977 (to be published); B. W. Lee, S. Pakvasa, R. E. Shrock, and H. Sugawara, *Phys. Rev. Lett.* **38**, 937 (1977).

⁷S. J. Barish *et al.*, *Phys. Rev. Lett.* **33**, 1446 (1974).

⁸See Ref. 3. There is a typographical error in the printing of Eq. (5) of that paper; the corrected equation should read $\theta_\gamma \approx \theta_L \sin \theta^*/(1 + \cos \theta^* - \theta_L^2/2)$.

⁹We reject at the scanning stage any obvious e^+e^- pair which points along the direction of a cosmic-ray shower or along the direction of a downgoing cosmic-ray muon, and is also within 20 cm of such a track.

¹⁰E. Bellotti, D. Cavalli, E. Fiorini, and M. Rollier, *Lett. Nuovo Cimento* **17**, 553 (1976).

Longitudinal-Transverse Separation for Inclusive Electroproduction of Pions and Protons*

C. J. Bebek, A. Browman,† C. N. Brown,‡ K. M. Hanson,† R. V. Kline, D. Larson,

F. M. Pipkin, S. W. Raither, A. Silverman, and L. K. Sistrerson§

Laboratory of Nuclear Studies, Cornell University, Ithaca, New York 14853, and High Energy Physics Laboratory, Harvard University, Cambridge, Massachusetts 02138

(Received 27 January 1977)

We use new measurements of the inclusive electroproduction reactions $eN \rightarrow e' \pi^\pm X$ and $eN \rightarrow e' p X$ with ϵ values in the range $0.35 < \epsilon < 0.45$ together with earlier measurements with $0.85 < \epsilon < 0.95$ to determine the contributions to the cross section due to transversely and longitudinally polarized photons in the range $1.2 \text{ GeV}^2 < Q^2 < 3.3 \text{ GeV}^2$. The longitudinal component is small and consistent with that observed in the total virtual-photoproduction cross section.

The longitudinal polarization of virtual photons provides a powerful probe for determining the spin of the constituents of the nucleon. For electroproduction experiments in which only the scattered electron is observed, the total virtual-photoproduction cross section can be written in the form

$$\sigma_{\text{tot}} = \sigma_T + \epsilon \sigma_L. \quad (1)$$

Here σ_T is due to transversely polarized photons, σ_L is due to longitudinally polarized photons, and ϵ is the polarization parameter for the virtual photons. The Stanford Linear Accelerator Center-Massachusetts Institute of Technology data give the value 0.14 ± 0.07 for the ratio $R = \sigma_L/\sigma_T$.¹ This small value of R is interpreted in the parton model to mean that the constituents are predominately spin- $\frac{1}{2}$ particles. This supports the quark

model for nucleon structure. The observed scaling of νW_2 and W_1 implies that R should be given by

$$R = Q^2/\nu^2 = 2M/\nu\omega, \quad (2)$$

where ν and $-Q^2$ are the energy and square of the mass of the virtual photon, respectively, and $\omega = 2M\nu/Q^2$. The available data are not sufficiently precise to distinguish between a constant R and a functional dependence of the form given by Eq. (2). There has been some speculation that the longitudinal component is due entirely to exclusive reactions such as $\gamma_{\nu p} \rightarrow \pi^+ n$ and that there is no longitudinal component in the inclusive reactions such as $\gamma_{\nu p} \rightarrow \pi^+ X$.²

In this Letter, we use new measurements made at low ϵ^{3A} of the inclusive electroproduction reac-

tions

$$eN \rightarrow e'\pi^+X \text{ and } eN \rightarrow e'pX, \quad (3)$$

together with earlier measurements⁵⁻⁸ to separate the contribution to the cross section due to transversely and longitudinally polarized photons in the range $1.2 \text{ GeV}^2 < Q^2 < 3.3 \text{ GeV}^2$. Reactions (3) can be analyzed in terms of the virtual-photon-production reactions

$$\gamma_\nu N \rightarrow \pi^+X \text{ and } \gamma_\nu N \rightarrow pX, \quad (4)$$

where the virtual photon's Q^2 , ν , ϵ , and direction are tagged by the scattered electron. The cross

$$E_h d^3\sigma/dp_h^3 = A + \epsilon C + \epsilon B \cos(2\varphi) + \left[\frac{1}{2}\epsilon(\epsilon + 1)\right]^{1/2} D \cos\varphi. \quad (6)$$

The four terms are the respective contributions from transverse photons, longitudinal photons, interference between the transverse amplitudes, and interference between longitudinal and transverse amplitudes. The polarization parameter ϵ is given in terms of laboratory variables by

$$\epsilon = \left\{ 1 + 2\left[\frac{\nu^2 + Q^2}{Q^2}\right] \tan^2\left(\frac{1}{2}\theta_e\right) \right\}^{-1}, \quad (7)$$

where θ_e is the electron scattering angle. ϵ is invariant under boosts along the direction of the virtual photon. The results presented here have been averaged over φ so as to eliminate the B and D terms in Eq. (6).

The data are presented in terms of $\langle f \rangle$ obtained by averaging the invariant cross section

$$f = E_h \frac{d^3\sigma}{dp_h^3} = \frac{2E_h^*}{p_{\text{max}}^*} \frac{d^3\sigma}{dx dp_T^2 d\varphi},$$

over the range $p_T^2 < 0.02 \text{ GeV}^2$ and $0 < \varphi < 2\pi$ and in terms of the invariant structure function $F(x, Q^2, W)$ obtained by averaging f/σ_{tot} over this same region. σ_{tot} is the total virtual-photon-production cross section. The proton total cross section, σ_p , was taken from a fit to the Stanford Linear Accelerator Center-Massachusetts Institute of Technology data.¹⁰ The neutron total cross section was assumed to be given by $\sigma_n = \sigma_p(1 - 0.75/\omega)$. The neutron results reported here were extracted from the deuterium data by assuming the deuteron to be the simple sum of a proton and neutron. $\langle f \rangle$ was integrated over the interval (x_1, x_2) to obtain

$$\bar{f} = \int_{x_1}^{x_2} \langle f \rangle dx = \bar{A} + \epsilon \bar{C}.$$

sections for Reactions (3) and (4) are related by⁹

$$d\sigma/d\Omega_e dE' dp_h^3 = \Gamma d^3\sigma/dp_h^3, \quad (5)$$

where h denotes the detected hadron and Γ is the "flux" of transversely polarized photons. The cross section $d^3\sigma/dp_h^3$ for Reactions (4) is a function of W (the center-of-mass energy), Q^2 , ϵ , p_T (the component of the hadron's momentum perpendicular to the direction of the virtual photon), $x = p_{\parallel}^*/p_{\text{max}}^*$ (the parallel component of the hadron's momentum normalized to the maximum possible momentum evaluated in the virtual-photon-target-nucleon center-of-mass system), and φ (the angle between the electron scattering plane and the virtual-photon-hadron plane).

The general form of the invariant virtual-photon-production cross section is

The two-arm spectrometer system described previously was used to take data at the (W, Q^2) points $(2.15 \text{ GeV}, 1.2 \text{ GeV}^2)$, $(2.65, 2.0)$, and $(2.65, 3.3)$ with a hydrogen target and at $(2.15, 1.2)$ with a deuterium target for values of ϵ in the range $0.35 < \epsilon < 0.45$.^{3,4} A similar spectrometer system was used in earlier experiments to take data at the same (W, Q^2) points with ϵ in the range $0.85 < \epsilon < 0.95$.⁵⁻⁸ In all three experiments a shower counter and a threshold Freon Cherenkov counter were used to identify scattered electrons. Pions and protons were separated by a threshold Freon Cherenkov counter for momenta greater than 1.8 GeV and by time of flight for smaller momenta. The low- ϵ data have been corrected for random coincidences ($\sim 1\%$), electronics dead time ($\sim 5\%$), target-wall background ($\sim 3\%$), absorption in counters ($\sim 5\%$), and electron misidentification ($\sim 1\%$). The high- ϵ data have also been corrected for random coincidences ($\sim 5\%$), electronics dead time ($\sim 5\%$), target-wall background ($\sim 5\%$), absorption in counters ($\sim 4\%$), and electron misidentifications ($\sim 2\%$). Pion decay losses were simulated in the Monte Carlo acceptance calculations of the spectrometers. Both spectrometers used in the low- ϵ experiment were checked with elastic electron scattering, and the mean ratios of the measured elastic scattering cross sections to the average of the world data for the electron and hadron arms were 0.972 ± 0.010 and 0.993 ± 0.004 , respectively. The overall systematic error of the low- ϵ experiment is estimated to be $\pm 7\%$. The spectrometers used in

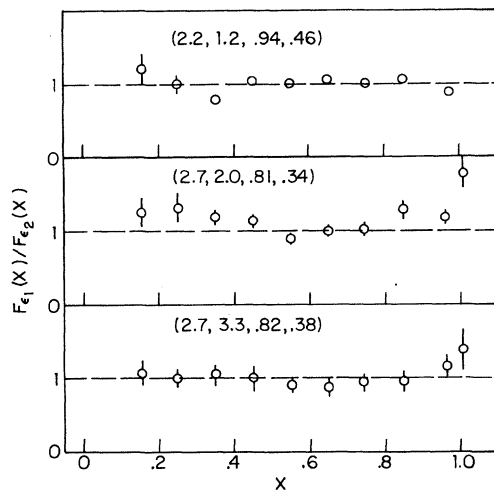


FIG. 1. Ratio of π^+ structure functions from a proton target for two values of ϵ at several $(W, Q^2, \epsilon_1, \epsilon_2)$ points.

the earlier high- ϵ experiments were also checked with elastic electron scattering measurements. The mean ratios of the measured elastic scattering cross sections to the average of the world data for the electron and hadron arms were 0.994 ± 0.007 and 0.998 ± 0.009 , respectively. The estimated systematic error in the high- ϵ data is also $\pm 7\%$. The same Faraday cup was used in both experiments. Since the two spectrometer systems were very similar and the procedures of data analysis were identical, we believe the systematic errors to be correlated such that the systematic uncertainties in \bar{A} and \bar{C} are $\pm 10\%$, one third of which is due to the uncorrelated portion of the systematic error. This uncorrelated portion introduces an uncertainty in $R = \bar{C}/\bar{A}$ of ± 0.06 . The errors shown in the figures and tables are statistical only and do not include the systematic errors.

Figures 1 and 2 show the ratio of the invariant structure function F for π^+ and π^- production from hydrogen as a function of x for two values of ϵ at the three (W, Q^2) points. The data show no trends and the ratios are consistent with being 1 over the range $0.1 < x < 0.8$. The region $x > 0.8$ is dominated by the resonances and the π^+ channel shows a particularly large longitudinal component.¹¹ A ratio of 1 indicates that the ratio of the longitudinal to transverse contributions for the inclusive cross section is the same as that found for the total virtual-photoproduction cross section. Similar results were obtained for the neutron-target data.

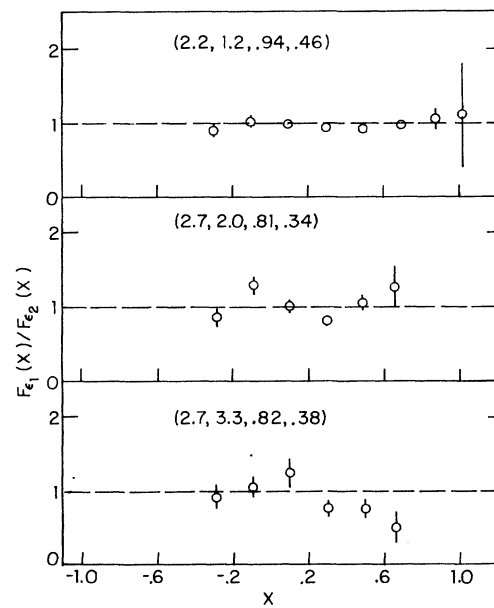


FIG. 2. Ratio of π^- structure functions from a proton target for two values of ϵ at several $(W, Q^2, \epsilon_1, \epsilon_2)$ points

Figure 3 shows the ratio of the invariant structure function for forward protons from a proton target. With the possible exception of the data at $Q^2 = 3.3 \text{ GeV}^2$ with $x > 0.2$, the ratio is consistent with 1 and indicates that the ratio of the longitudinal to the transverse component is the same as

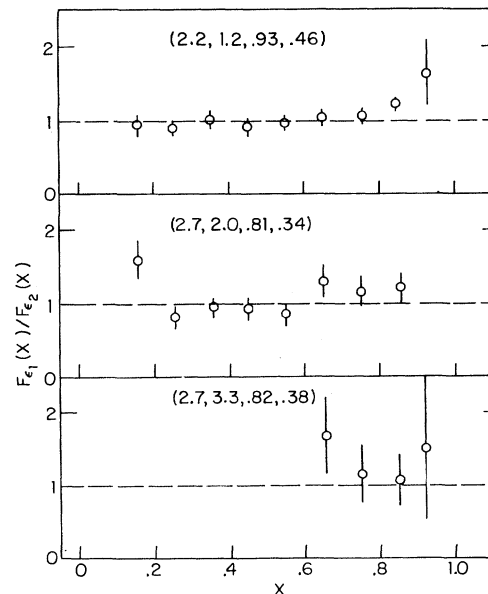


FIG. 3. Ratio of proton structure function from a proton target for several $(W, Q^2, \epsilon_1, \epsilon_2)$ points.

TABLE I. Pion separation results for $0.3 < x < 0.7$ and proton separation results for $0.0 < x < 1.0$.

TARGET	W (GeV)	Q ² (GeV ²)	ϵ_1	ϵ_2	π^+		π^-		p		
					$\frac{\bar{A}+\epsilon_1\bar{C}}{\bar{A}+\epsilon_2\bar{C}}$	$\frac{\bar{C}}{\bar{A}}$	$\frac{\bar{A}+\epsilon_1\bar{C}}{\bar{A}+\epsilon_2\bar{C}}$	$\frac{\bar{C}}{\bar{A}}$	$\frac{\bar{A}+\epsilon_1\bar{C}}{\bar{A}+\epsilon_1\bar{C}}$	$\frac{\bar{C}}{\bar{A}}$	
p	2.15	1.2	0.94	0.45	0.99±0.05	-0.02					
						+0.11					
						-0.10					
						+0.14					
p	2.70	2.0	0.81	0.34	1.15±0.05	0.36	1.02±0.09	0.04	+0.22	1.04±0.05	0.09
						-0.13			-0.19		-0.11
						+0.21			+0.64		+0.34
						-0.19			-0.42		-0.27
p	2.70	3.3	0.82	0.38	1.05±0.08	0.12	0.91±0.26	-0.19	+0.19	1.09±0.11	0.23
						+1.61			+0.19		+0.59
						-0.80			-0.16		-0.41
n	2.15	1.2	0.94	0.45	1.32±0.26	0.93	0.97±0.09	-0.06	+0.09	1.22±0.15	0.57
						+0.09			+0.09		+0.06
						-0.09			-0.08		-0.06
d	2.15	1.2	0.94	0.45	1.05±0.04	0.11	1.00±0.04	0.00		1.00±0.03	0.00

that found for the total virtual-photoproduction cross section. Similar results were obtained for the neutron-target data.

Table I summarizes the ratios of \bar{f} and \bar{C}/\bar{A} for the pion data in the region $0.3 < x < 0.7$ and for the proton data in the region $0.0 < x < 1.0$. Within errors the longitudinal-transverse ratio is consistent with zero and also with the value observed for the total virtual-photoproduction cross section. The average \bar{C}/\bar{A} for the three (W , Q^2) points from hydrogen are 0.09 ± 0.07 , 0.08 ± 0.12 , and -0.05 ± 0.05 for π^+ , π^- , and protons, respectively. We have estimated the effects of electron radiative corrections on the ratios in Table I. The effect on the ratio of \bar{f} 's is less than 1%.

In summary, we have studied the ratio of the longitudinal and transverse cross sections for the inclusive electroproduction of forward charged pions and forward protons from proton and neutron targets. The longitudinal component is small and is consistent with either being zero or being the same as that found for the total virtual-photoproduction cross section.

We wish to acknowledge the support of Professor Boyce McDaniel, the staff of the Wilson Synchrotron Laboratory, and the staff of the Harvard High Energy Physics Laboratory.

*Research supported in part by the U. S. Energy Research and Development Administration (Harvard University) and in part by the National Science Foundation (Cornell University).

†Present address: Clinton P. Anderson Laboratory, Los Alamos, N. Mex. 87545.

‡Present address: Fermi National Accelerator Laboratory, P. O. Box 500, Batavia, Ill. 60510.

§Present address: 36 Webb Street, Lexington, Md. 02173.

¹R. E. Taylor, in *Proceedings of the International Symposium on Lepton and Photon Interactions at High Energy, Stanford, California, 1975*, edited by W. T. Kirk (Stanford Linear Accelerator Center, Stanford, Calif., 1976), p. 679.

²H. Harari, in *Proceedings of the International Symposium on Electron and Photon Interactions at High Energies, Ithaca, New York, 1971*, edited by N. B. Mistry (Laboratory of Nuclear Studies, Cornell University, Ithaca, N. Y., 1972), p. 299.

³C. J. Bebek *et al.*, Phys. Rev. Lett. **37**, 1525 (1976).

⁴C. J. Bebek *et al.*, to be published.

⁵C. J. Bebek *et al.*, Phys. Rev. Lett. **30**, 624 (1973), and Nucl. Phys. **B75**, 20 (1974).

⁶C. J. Bebek *et al.*, Phys. Rev. Lett. **32**, 27 (1974).

⁷C. J. Bebek *et al.*, Phys. Rev. Lett. **34**, 749 (1975).

⁸C. J. Bebek *et al.*, Phys. Rev. Lett. **34**, 1115 (1975).

⁹L. Hand, Phys. Rev. **129**, 1834 (1963).

¹⁰W. B. Atwood, private communication.

¹¹C. J. Bebek *et al.*, Phys. Rev. Lett. **37**, 1326 (1976).